HHS Public Access

Author manuscript

F S Sci. Author manuscript; available in PMC 2024 May 16.

Published in final edited form as:

F S Sci. 2022 May ; 3(2): 118–129. doi:10.1016/j.xfss.2022.03.002.

The role of Hippo pathway signaling and A-kinase anchoring protein 13 in primordial follicle activation and inhibition

Jacqueline Yano Maher, M.D.[a,b,c], **Md Soriful Islam, Ph.D.**[a], **Ophelia Yin, M.D.**[d], **Joshua Brennan, M.P.H., M.S.**[a], **Ethan Gough, Ph.D.**[e], **Paul Driggers, Ph.D.**[a], **James Segars, M.D.**[a]

[a]Johns Hopkins School of Medicine, Baltimore, Maryland

[b]Eunice Kennedy Shriver National Institute of Child Health and Human Development, National Institutes of Health, Bethesda, Maryland

[c]Children's National Medical Center, Washington, D.C.

[d]David Geffen School of Medicine, University of California, Los Angeles, California

[e]Department of International Health, Johns Hopkins Bloomberg School of Public Health, Baltimore, Maryland

Abstract

Objective: To determine whether the mechanotransduction and pharmacomanipulation of A-kinase anchoring protein 13 (AKAP13) altered Hippo signaling pathway transcription and growth factors in granulosa cells. Primary ovarian insufficiency is the depletion or dysfunction of primordial ovarian follicles. In vitro activation of ovarian tissue in patients with primary ovarian insufficiency alters the Hippo and phosphatase and tensin homolog/phosphatidylinositol 3-kinase/protein kinase B/forkhead box O3 pathways. A-kinase anchoring protein 13 is found in granulosa cells and may regulate the Hippo pathway via F-actin polymerization resulting in altered nuclear yes-associated protein (YAP)/transcriptional coactivator with PDZ-binding motif coactivators and Tea domain family (TEAD) transcription factors.

Design: Laboratory studies.

Setting: Translational science laboratory.

Patient(s): None.

Intervention(s): COV434 cells, derived from a primary human granulosa tumor cell line, were studied under different cell density and well stiffness conditions. Cells were transfected with a TEAD-luciferase (TEAD-luc) reporter as well as expression constructs for AKAP13 or AKAP13 mutants and then treated with AKAP13 activators, inhibitors, and follicle-stimulating hormone.

Main Outcome Measure(s): TEAD gene activation or inhibition was measured by TEAD-luciferase assays. The messenger ribonucleic acid levels of Hippo pathway signaling molecules,

Reprint requests: Jacqueline Y. Maher, M.D., Division of Pediatric and Adolescent Gynecology, Eunice Kennedy Shriver National Institute of Child Health and Human Development, National Institutes of Health, 10 Center Dr. Rm. 8N248 MSC 1840, Bethesda, Maryland 20892 (jacqueline.maher@nih.gov).

J.Y.M. has nothing to disclose. M.S.I. has nothing to disclose. O.Y. has nothing to disclose. J.B. has nothing to disclose. E.G. has nothing to disclose. P.D. has nothing to disclose. J.S. has nothing to disclose.

including *connective tissue growth factor (CTGF)*, *baculoviral inhibitors of apoptosis repeat-containing 5*, *Ankyrin repeat domain-containing protein 1*, *YAP1*, and *TEAD1*, were measured by quantitative real-time polymerase chain reaction. Protein expressions for AKAP13, CTGF, YAP1, and TEAD1 were measured using Western blot.

Result(s): Increased TEAD-luciferase activity and expression of markers for cellular growth were associated with decreased cell density, increased well stiffness, and AKAP13 activator (A02) treatment. Additionally, decreased TEAD-luc activity and expression of markers for cellular growth were associated with AKAP13 inhibitor (A13) treatment, including a reduced expression of the *BIRC5* and *ANKRD1* (YAP-responsive genes) transcript levels and CTGF protein levels. There were no changes in TEAD-luc with follicle-stimulating hormone treatment, supporting Hippo pathway involvement in the gonadotropin-independent portion of folliculogenesis.

Conclusion(s): These findings suggest that AKAP13 mediates Hippo-regulated changes in granulosa cell growth via mechanotransduction and pharmacomanipulation. The AKAP13 regulation of the Hippo pathway may represent a potential target for regulation of follicle activation.

Keywords

Premature ovarian insufficiency; primordial follicle activation; AKAP13; Hippo pathway; granulosa cell

Human females are born with a set number of eggs, starting with a maximum of 6–7 million eggs, which decline over time to 1 million at birth, 300,000–500,000 at puberty, 25,000 at the age of 37 years, and 1,000 at menopause (1). Primary ovarian insufficiency (POI), also known as premature ovarian insufficiency or premature ovarian failure, is a devastating diagnosis that affects approximately 1% of women aged <40 years. Primary ovarian insufficiency is a result of early ovarian follicle depletion or dysfunction (2, 3), where women aged ≤40 years have amenorrhea for ≥4 months and elevated serum follicle-stimulating hormone (FSH) levels in the menopausal range measured twice at least 1 month apart (4, 5).

Primordial follicles are a dormant type of follicle composed of an oocyte arrested at prophase I and surrounded by a single layer of squamous granulosa cells; these follicles reside in the gonadotropin-independent portion of folliculogenesis. It is known that multiple paracrine factors between the granulosa cells and the oocyte in addition to intracellular signaling pathways are involved in follicular growth. However, the mechanism of selection and activation of some of the primordial follicles while others remain dormant into adulthood remains unclear (6). Primordial follicle activators that have been studied include the following (7): phosphatase and tensin homolog (PTEN) inhibitors/protein kinase B (Akt) stimulators (8-12); BMP4/7 (13-15); GDF-9 (13-15); KIT ligand (16, 17); FGF2/7 (18, 19); insulin (20, 21); GREM1/2 (22, 23); and Leukemia inhibitory factor (24). Primordial follicle inhibitors that have been reported include the following (7): yes-associated protein (YAP)/Hippo signaling disruptors (9); anti-Müllerian hormone (25); mTORC1/2 inhibitors (26-28); and forkhead box O3 (FOXO3) (25, 29). Understanding how to manipulate primordial

follicles by inhibition and activation could assist women with few remaining follicles achieve pregnancy, such as those with POI.

Clinical research in the treatment of young women with idiopathic POI has shown that removal of the ovaries or ovarian cortex followed by in vitro activation (IVA) and reinsertion of the tissue has resulted in approximately 10 live births (30). In vitro activation was developed on the basis of knowledge of altering 2 pathways: the Hippo signaling pathway (31, 32), which is involved in tumor suppression, and the PTEN/phosphatidylinositol 3-kinase (PI3K)/protein kinase B (Akt)/FOXO3 pathway, which is involved in cancer cell proliferation. Thus, manipulating these pathways via tissue fragmentation and culturing with PTEN inhibitors and PI3K stimulators (33, 34) have been shown to have implications in primordial follicle dormancy and activation. Focusing on the Hippo pathway, IVA by ovarian tissue fragmentation is thought to alter cell to cell contact and extracellular matrix (ECM) rigidity. Because primordial follicles are predominantly found in the ovarian cortex, which is collagen-rich and more rigid than the softer medulla where they migrate as they develop (35, 36), the matrix rigidity likely plays a role in the dormant vs. proliferative state of the ovarian follicle. In vitro activation affects mechanotransduction by altering Rho GTPase activity and F-actin polymerization, which disrupts Hippo pathway gene expression. This causes levels of cytoplasmic stimulatory transcriptional coactivators YAP and transcriptional coactivator with PDZ-binding (postsynaptic density protein 95, Drosophila disc large tumor suppressor, and zona occludens 1) motif (TAZ) to increase in the cytoplasm; the factors move to the cell nucleus; bind to Tea domain family (TEAD) transcription factors (TEAD1–4), a highly conserved deoxyribonucleic acid (DNA) binding domain; and increase in the transcription of growth factors, including CCN (CYR61, connective tissue growth factor [CTGF], and nephroblastoma overexpressed proteins) and baculoviral inhibitors of apoptosis repeat containing (BIRC). These changes in mechanotransduction, active YAP/TAZ quantities, and TEAD expression lead to cell proliferation (37) and folliculogenesis (38). In contrast, if YAP is converted to inactive phosphorylated YAP (pYAP), it is then degraded, and transcription of growth factors does not take place.

As stated earlier, 10 births have been reported by IVA by altering the Hippo and PTEN/PI3K/Akt/FOXO3 pathways. The first live births were from 2013 to 2016, when Kawamura et al. (9), Suzuki et al. (39), and Zhai et al. (40) used IVA in ovarian tissue from women with POI; they fragmented fresh or frozen/thawed tissue to disrupt the Hippo pathway and then treated the tissue with PI3K stimulators and PTEN inhibitors. From these 3 studies in 51 patients, 15 women had follicular development, 3 had live births and 1 had a miscarriage (9, 39, 40). Additionally, a study using a drug-free approach with fragmentation alone reported 1 case of an ongoing pregnancy in a patient with POI (41). In a similar fashion, drug-free IVA was performed in 11 patients with poor ovarian reserve and resulted in 1 live birth, 2 ongoing pregnancies, and 1 miscarriage (42). To expand on concepts from these studies, the current study hypothesized that changes in cell density and matrix composition in cell culture would alter the Hippo pathway by mechanotransduction and new pharmacologic treatments could alter the Hippo pathway and potentially act as primordial follicle activators and inhibitors (Supplemental Fig. 1, available online).

A-kinase anchoring protein 13 (AKAP13) is a member of the AKAP family of proteins, which is comprised of over 40 functionally related genes notable for their multiple binding domains. A-kinase anchoring protein 13 is expressed in the cytoplasm of granulosa cells in mature follicles, the corpus luteum, and hilar cells in the ovary (43). Our group previously cloned the full-length transcript of this novel protein AKAP13, which was known to regulate protein kinase A (PKA) (44). A-kinase anchoring protein 13 has multiple domains that allow for cascades of reactions and downstream hormone signaling (45). A-kinase anchoring protein 13 contains a PKA regulatory subunit II (PKA RII) binding domain at its N-terminus, and PKA is downstream of FSH signaling. The guanine nucleotide exchange factor (GEF) domain (44, 46, 47) is in the mid region, and a nuclear receptor interaction domain is located in a region in the C-terminus. The GEF domain activates small guanosine-5′-triphosphate (GTP)-binding proteins, such as Ras homolog family member A (RhoA), which belongs to the Rho family of small GTPases that function as molecular switches between the inactive GDP- and active GTP-bound states, regulating cell differentiation, proliferation, movement (48, 49), and actin nucleation (50). Microfilaments and their proportion of F-actin to G-actin have been shown to affect primordial follicle activation through Hippo signaling inhibition. An increase in F-actin disrupts the Hippo pathway, leading to an increase in stimulatory YAP protein and downstream follicular growth (9). Rho activation by AKAP13 and its effect on the Hippo pathway via YAP/TAZ activity have also been described in human embryonic stem cell survival (51). This interaction of the AKAP13 GEF region, F-actin, and the Hippo pathway was the focus of this study.

A-kinase anchoring protein 13 indirectly affects Hippo pathway activity because it influences RhoA and F-actin, which are upstream of the Hippo pathway genes that negatively regulate YAP/TAZ transcriptional coactivators (Fig. 1, Graphical Abstract). Diviani et al. (52) identified several small anionic compounds, including molecules A13 and A02, that interact with the DH domain in the GEF region of AKAP13, which alters the oncogenic Rho signaling and catalytic activity of AKAP13 (Supplemental Fig. 2, available online). A13 was found to inhibit AKAP13 by >90% in a human kidney cell line and reduce cell proliferation, migration, and invasion of prostate cancer cells (52). The effects of A13 and these molecules have not yet been tested in granulosa cells; thus, A13 was chosen for its possible inhibitory effects, and A02 was chosen for its potential activating effects.

To expand on prior research, this study hypothesized that the mechanotransduction and pharmacomanipulation of AKAP13 could modulate the Hippo signaling pathway and significantly alter granulosa cell transcription factors and growth factors. To test this hypothesis, COV434 cells, derived from a primary human granulosa tumor cell line, were used with a TEAD-luciferase (TEAD-luc) reporter assay, quantitative real-time polymerase chain reaction (qPCR), and immunoblotting as a model to study the effects of Hippo pathway manipulation. These experiments sought to probe the influence of cell density and matrix composition as well as the role of AKAP13 on the Hippo pathway with the use of an AKAP13 inhibitor (A13) and an AKAP13 activator (A02) in a human granulosa cell line. With a deeper understanding of primordial follicle activation and inhibition via the Hippo pathway and AKAP13, future research may probe alterations in AKAP13 as a potential target for regulation of follicle growth and a potential treatment for POI.

MATERIALS AND METHODS

The following experiments were entirely completed with cell lines. No humans or animals were involved; therefore, the study did not need to be reviewed or approved by the Johns Hopkins Institutional Review Board.

Cell Line

COV434 cells (Sigma-Aldrich, St. Louis, MO; #07071909) are a diploid immortalized human granulosa cell line derived from a granulosa cell tumor and have been demonstrated to be hormonally responsive (53).

Cell Culture and Plating

COV434 cells were cultured in fresh Dulbecco's Modified Eagle Medium (Thermo Fisher Scientific, Waltham, MA) supplemented with 10% fetal bovine serum (FBS) (GIBCO by Life Technologies, Carlsbad, CA) with 1% penicillin/streptomycin (MilliporeSigma, Burlington, MA; #P3032-10MU/#S9137-25G) and 1% L-glutamine (Quality Biological, Gaithersburg, MD) at 37 °C in 95% air-5% CO_2. Cells were stained with trypan blue (Sigma-Aldrich) to assess viability and were counted using an automated cell counter (NanoEnTek Eve Automatic Cell Counter; NanoEnTek, Seoul, Korea). For most experiments, the cells were plated on collagen I-coated polystyrene plates (2–4 GPa) (Corning, Corning, NY) in varying well size plates, including 12-, 24-, and 48-well plates.

To evaluate the effects of the ECM on mechanotransduction due to matrix stiffness and coating components, cells were plated on 4 different types of plates: stiff collagen I-coated polystyrene plates (2–4 GPa) (Corning) and 3 types of soft silicone plates for comparison (930 KPa) (Flexcell International, Burlington, NC)—untreated, laminin-coated, and ProNectin-coated. The ECM has an important role in ovarian function and cell growth and development and contains collagens I, III, IV, and VI, laminin, and fibronectin (54-57). In bovine ovaries, laminin is found in low levels within the granulosa cell compartment of the follicle but is highly localized in the basal lamina as a defined ring exterior to the follicular granulosa cell (54, 55). Laminin has also been found in human granulosa cells that were cultured after in vitro fertilization oocyte retrieval (58). Fibronectin is commonly found in stromal ECM and is important for cell migration, which occurs during follicle expansion and development. Fibronectin has been shown to be produced and secreted by rat and bovine granulosa cells (56, 59, 60) and has increased levels in the theca cell compartment and follicular fluid of mouse follicles (55). ProNectin is a biosynthetic polymer that contains the tripeptide Arg-Gly-Asp ligand of human fibronectin, which is also found in the ECM.

Transfection of COV434 Cells

Plasmids

TEAD-luciferase.: In the Hippo pathway, YAP and TAZ coactivators bind to the TEAD transcription factors (TEAD1-4). Because TEADs mediate nuclear YAP/TAZ function in transcriptional activation, a transient transfection TEAD-luc reporter (TEAD-luc = 8xGTIIC-luc) (Sigma-Aldrich; #34615) (37) construct was used as a proxy for gene activation by YAP/TAZ (Supplemental Fig. 3, available online). TEAD-luciferase activity

was used to interpret changes in intranuclear YAP/TAZ and messenger ribonucleic acid (mRNA) transcription, which are upstream to growth factors BIRC and CTGF.

AKAP13.: A complementary DNA (cDNA) encoding the N-terminal coding sequences of *AKAP13* and overlapping with the *BRX* cDNA sequence (GenBank entry AF126008) was amplified from a human mammary gland Marathon-Ready cDNA library (Clontech, Mountain View, CA) and subcloned into an expression vector for Brx (61). Expression constructs for the 1.8-kb human AKAP13 were used in transfection experiments to overexpress AKAP13 (62).

HMax-AKAP13.: The complete cDNA sequence encoding AKAP13 was subcloned into a pcDNA4/HisMaxC (Invitrogen, Carlsbad, CA) expression vector to generate HMax-AKAP13 (HMax) and confirmed by next-generation sequencing. HMax was transfected as an empty vector control.

AKAP13 mutants RII(-) and GEF(-).: Protein kinase A subunits are expressed in the ovary (63), and the RII subunit, specifically, is up-regulated in response to FSH (64, 65). A-kinase anchoring protein 13 contains a PKA RII binding domain at its N-terminal. Mutant versions of AKAP13 were derived from the wild-type AKAP13 cDNA by overlap amplification with primers containing site-specific mutations. The PKA RII-AKAP13 mutant, RII(-), was created via the introduction of 2 point mutations: alanine to proline at position 1251 and isoleucine to proline at position 1260 (A1251P/I1260P). This mutant disrupts binding of the PKA RII regulatory subunit to AKAP13, thus interfering with activation of PKA by AKAP13 (66). The GEF domain is capable of binding to RhoA (44, 46, 47). Activation of RhoA can lead to cytoskeletal rearrangement and cellular proliferation. The GEF-AKAP13 mutant, GEF(-), which has a tyrosine to phenylalanine substitution at amino acid 2153 (Y2153F) located within the GEF region, was constructed to cause inactivation of GEF activity in the wild-type AKAP13 (67).

FSH receptor.: The FSH receptor (FSHR) is a wild-type N-terminal 3xHA-tagged human follitropin receptor cloned into pcDNA3.1+ (Invitrogen) at EcoRI (5′) and XhoI (3′). The FSHR was obtained from the cDNA Resource Center (www.cdna.org, GenBank accession #AY429104). COV434 cells are a useful model because they are similar to primordial follicle granulosa cells that are not responsive to gonadotropins but have preservation of gonadotropin-independent Hippo signaling. The FSHR is endogenously expressed in COV434 cells but is nonfunctional because it is uncoupled from downstream signaling. COV434 cells only become FSH responsive if the FSHR is transfected into the cells.

Transfection, cell lysis, and luciferase assay.—COV434 cells were plated at a density dependent on the size of the well for each experiment resulting in approximately 50%–70% confluence the next day. Using a 2-day modified reverse transfection method, cells were plated and immediately transfected with TEAD-luc and other vectors using FuGENE 6 (Roche Molecular Biochemicals, Pleasanton, CA), as described by the manufacturer. On day 2, MTS solution (Promega, Madison, WI) was added for normalization of the number of viable cells per well, and an absorbance of 490 nm was measured on a CLARIOstar Microplate Reader machine (BMG Labtech, Cary, NC) per

the manufacturer's instructions. Subsequently, cells were lysed, and luciferase activity was assessed using a Firefly luciferase (LUC I) assay kit (Promega). TEAD-luciferase activity was measured using a CLARIOstar Microplate Reader in relative light units (RLUs).

A13 or A02 treatment of cell culture.—A13 and A02 are small molecules previously identified by virtual screening for molecules that altered the Rho-GEF activity of AKAP13 (52) (Supplemental Fig. 2). These molecules were used to manipulate the Hippo pathway pharmacologically via AKAP13. A13 (ChemBridge, San Diego, CA; Cat #7390017) is a small protein-protein interaction inhibitor of AKAP13, and A02 (Ambinter, Orléans, France; Cat #Amb20267665) is a small protein-protein interaction activator of AKAP13. They interact with the DH domain in the GEF region of AKAP13. A13 halts the oncogenic Rho activation of AKAP13. In contrast, A02 binds to the GEF region of AKAP13 and activates the Rho enzymatic activity of AKAP13. As described in the following, a 4-day protocol was used, and COV434 cells were treated with 10 μM of A13 or 10 μM of A02 for 24 hours.

FSH treatment of cell culture.—To assess gonadotropin independence vs. dependence, in some experiments, a 4-day protocol was used to incorporate Sodium Chloride (NaCl) or FSH treatment. On day 1, cells were plated at 200×10^3 cells/well. On day 2, after 24 hours of culture in 10% FBS media, cells were approximately 20%–40% confluent and were then serum-starved with medium containing 0.5% FBS. On day 3, after 24 hours of cell starvation, cells were 40%–60% confluent and transfected with the TEAD-luc reporter and FSHR plus one of the following expression vectors: HMax, an empty vector; AKAP13; AKAP13 PKA RII(-) mutant; or AKAP13 GEF(-) mutant, using FuGENE 6. In some experiments, 10 μM of A13 or 10 μM of A02 treatment was added to wells immediately following this step. Four hours after transfection, cells received additional treatment of 1 IU of FSH (GONAL-f; Merck Serono, Darmstadt, Germany) or 0.9% NaCl, as a control. On day 4, 24 hours after transfection, MTS and TEAD-luc assays were performed.

Well Size

As a first step in examining cell signaling and TEAD-luc activity, COV434 cells were plated at 240×10^3 cells/well in 3 differently sized (48, 24, and 12) well plates. Thus, the lower the well plate number, the greater the well size, and the lower the cell density. The total volume per well included the following: 48 wells, 200 μL/well; 24 wells, 500 μL/well; and 12 wells, 1,000 μL/well. Using a modified reverse transfection protocol, cells were transfected with TEAD-luc. After 24 hours, cells were lysed and assayed for luciferase activity.

Well Stiffness

To evaluate differences in well stiffness and composition, changes in TEAD-luc activity among stiff polystyrene (2–4 GPa) vs. 3 different soft silicone plates (930 KPa) (Flexcell plates: untreated, laminin-coated, or ProNectin-coated) were assessed.

Replicates and Data Calculations for Luciferase Assays

Experiments each had multiple technical replicates (4 in 48-well plates, 3 in 24-well plates, 2 in 12-well plates, and 3 in 6-well plates). Each experiment had 2–3 biologic replicates performed. Specifics are described in each figure legend. For luciferase assays, RLUs were

corrected for by the MTS cell viability assay (TEAD-luc RLU divided by MTS) or protein level with precision red (Thermo Fisher Scientific; Cat #NC9542014) (TEAD-luc RLU divided by protein). Fold change was calculated by dividing each corrected value by the control condition for each experiment.

Quantitative Real-Time Polymerase Chain Reaction

COV434 cells were cultured in 60-mm dishes or 6-well plates, and approximately 50% confluent cells were treated with 10 μM of A13 or vehicle control (dimethyl sulfoxide) for 24 hours. Cells were lysed with RLT buffer and purified with an RNeasy Mini Kit (Qiagen, Germantown, MD). The level and purity of RNA were measured with the NanoVue Plus (Bio-chrom US, Holliston, MA). The RNA was converted to cDNA (50–100 ng/μL) using the iScript cDNA Synthesis Kit (Bio-Rad, Hercules, CA) in a Bio-Rad Thermocycler machine. Quantitative real-time polymerase chain reaction was performed on LightCycler 96 System (Roche Diagnostics, Mannheim, Germany) in a 96-well plate with 4 ng/μL of cDNA in a final volume of 10 μL containing 1X FastStart Essential DNA Green Master (Roche Diagnostics, Indianapolis, IN), with appropriate primer sets of selected Hippo pathway target genes, including *CTGF*, *BIRC5*, *ANKRD1*, *YAP1*, and *TEAD1* (Supplemental Table 1, available online). *CTGF*, also known as *CCN2*, a known direct TAZ-TEAD target gene, is one of the main players in tissue remodeling and fibrosis. *BIRC5* (also known as survivin) is a YAP-responsive gene (68), which is known to inhibit apoptosis and promote cell proliferation (69). Additionally, *ANKRD1* (ankyrin repeat domain 1) is another YAP-responsive gene (70), and its overexpression is associated with antiapoptosis and epithelial-mesenchymal transition features (71). Primers were purchased from Integrated DNA Technologies (Coralville, IA). The housekeeping gene *RPLP0* was amplified under the same conditions for normalizing quantitative data. The relative mRNA expression was calculated using the ΔΔCT method (72) and is presented as fold increase or decrease relative to control.

Western Blot

COV434 cells were cultured on a 60-mm dish or a 6-well plate. At approximately 50% confluence, cells were left untreated, transfected with empty vector HMax, or transfected with AKAP13 for over expression, or treated with A13 at 10 or 20 μM for 24 hours. Cells were washed with phosphate-buffered saline and lysed with radioimmunoprecipitation assay buffer (Sigma-Aldrich; #R0278) containing protease and phosphatase inhibitor cocktail (Thermo Fisher Scientific). The protein levels were quantified using the Pierce BCA Protein Assay Kit (Thermo Fisher Scientific). Equal volumes (30–40 μg) of protein lysates were loaded onto 4%–12% NuPAGE gels (Thermo Fisher Scientific) and resolved by sodium dodecyl sulfate polyacrylamide gel electrophoresis under reducing conditions and then transferred to 0.2-μm nitrocellulose membranes in an XCell II apparatus (Thermo Fisher Scientific). Ponceau S Solution (Sigma-Aldrich; #P7170) was used for the detection of protein on nitrocellulose membranes. After blocking membranes with 5% nonfat milk with Tris-buffered saline (1X) with Tween 20 (0.1%) (TBST) for 1 hour, membranes were incubated overnight at 4 °C with primary antibodies including AKAP13, CTGF, non-pYAP, TEAD1, and β-actin (Supplemental Table 2, available online) diluted in 5% bovine serum albumin with TBST. To prepare anti-AKAP13, rabbit primary antisera were directed

against AKAP13, and a peptide corresponding to AKAP13 was used to generate polyclonal antiserum 6969 using standard techniques. A-kinase anchoring protein 13 binding was confirmed using enzyme-linked immunosorbent assay (Covance Laboratories, Gaithersburg, MD) (73). On the next day, membranes were washed 3 times (5 minutes for each wash) with TBST and then incubated with appropriate horseradish peroxidase-conjugated secondary antibodies as 1:10,000 dilutions (GE Healthcare, Chicago, IL; #NA934V or NA931V) with 5% nonfat milk with TBST for 2 hours at room temperature. Subsequently, membranes were washed 3 times (5 minutes for each wash) with TBST, and immunoreactive proteins were visualized using a SuperSignal West Pico Plus Chemiluminescent Substrate (Thermo Fisher Scientific) in an Azure Imager c300 system (Azure Biosystems, Dublin, CA). The band intensity was quantified using ImageJ software (version 1.52a) and normalized against corresponding anti-β-actin.

Statistics

Statistical analyses were performed using Prism 5 software (GraphPad Software, Inc., La Jolla, CA) or R version 4.0.2. The number of replicates is indicated in the individual figure legends. The results of luciferase assays and sample values are presented as mean ± standard error of the mean. Fold changes were used to compare experimental data results. In the cell density and matrix stiffness experiments (Fig. 3A and B), a Kruskal-Wallis test was performed with a post hoc Mann-Whitney U test. In the AKAP13 manipulation experiments (Fig. 4A and B), a permutation 2-way analysis of variance (ANOVA) was performed with post hoc quantile 1-way ANOVA to compare each pair of experimental groups where the permutation 2-way ANOVA results were statistically significant. Data are presented with false discovery rate-adjusted P values. For qPCR, 1-way quantile ANOVA was used for analyses. Differences were considered statistically significant at $P \leq .05$.

RESULTS

Protein Expression of Endogenous AKAP13 in COV434 Cells

Western blotting for protein expression indicated that detectable endogenous AKAP13 was present in COV434 cells that were untransfected, or transfected with empty expression vector, HMax. The results showed that with transfection of an AKAP13 vector, AKAP13 was expressed at higher levels in human granulosa cells (Supplemental Fig. 4, available online).

Changes in Cell Density Increase TEAD Signaling

To simulate ovarian tissue fragmentation, cell density was decreased by plating the same number of cells in wells of increasing sizes, resulting in an increase in TEAD-luc activity (Supplemental Fig. 5, available online). From 48- to 24-well plates, 24- to 12-well plates, and 48- to 12-well plates, COV434 cells demonstrated a 2.8-fold ($P < .001$), 3.7-fold ($P < .001$), and 10.4-fold ($P < .001$) higher TEAD-luc activity, respectively (Fig. 2A).

An Increase in Well Stiffness Increases TEAD Signaling

To evaluate changes in mechanotransduction signaling, 4 different types of plates were compared. There was a significant decrease in TEAD-luc activity between the polystyrene

plate and all 3 silicone Flexcell plates. Polystyrene is the typical well type with a rigidity of 2–4 GPa. The Flexcell plates were 930 KPa with different coatings: untreated; laminin; and ProNectin. There was a significant decrease in TEAD-luc activity between the polystyrene plate and all 3 silicone Flexcell plates ($P < .0001$), meaning that there were greater reporter activity in cells plated on a stiffer matrix and increased mechanotransduction. There was no significant difference between untreated Flexcell plates and laminin- or ProNectin-coated plates ($P = .24$ and $P = .13$, respectively) (Fig. 2B).

AKAP13 Mutant Transfection and FSH Treatment Did Not Affect Gonadotropin-Independent Folliculogenesis

To evaluate the effects of various AKAP13 expression levels and FSH response on the Hippo pathway, COV434 cells were transfected with empty vector HMax, AKAP13 overexpression, AKAP13 mutant GEF(-), and AKAP13 mutant RII(-) and then treated with 0.9% NaCl or 1 IU of FSH and analyzed with TEAD-luc. There were no statistically significant differences in TEAD-luc expression for the overall experiment or for each of the paired transfection comparisons between NaCl and FSH treatment. There were also no differences between empty vector HMax, AKAP13 overexpression, and GEF(-) or RII(-) mutant transfected cells treated with NaCl (Fig. 3A).

Changes in Hippo Pathway Growth Factors Induced by Pharmacologic Inhibitors and Activators of AKAP13

To compare the effects of A13 and A02 on the Hippo pathway, TEAD-luc activity was compared between empty vector HMax transfection, AKAP13 transfection for overexpression, treatment with 10 μM of A13, and treatment with 10 μM of A02. For each of these conditions, 0.9% NaCl or 10 μM of FSH was added 4 hours later. Addition of AKAP13 did not augment TEAD-luc reporter activity, possibly due to high levels of endogenous AKAP13 in COV434 cells. Treatment with A13 reduced TEAD-luc activity by 68% ($P < .0001$), and treatment with A02 increased TEAD-luc activity by 73% ($P < .0001$). FSH treatment or vehicle control did not affect TEAD-luc reporter activity (Fig. 3B).

To evaluate whether A13 had effects on RNA and protein, qPCR was used to test the effects of A13 on Hippo signaling cascades in COV434 immortalized human granulosa cells. To assess whether AKAP13 and RhoA were involved in Hippo/YAP signaling in granulosa cell function, A13, an inhibitor of the interaction between AKAP13 and RhoA (52), was used. COV434 granulosa cells were treated with A13 at 10 or 20 μM for 24 hours to measure the mRNA or protein levels of several components of Hippo signaling. Growth factor CTGF, also known as CCN2, is important for tissue growth and remodeling (74). The mRNA levels of *CTGF* were not affected (Fig. 4A), whereas the protein levels of CTGF (Fig. 4B) were greatly reduced by A13 treatment in granulosa cells compared with those in untreated control. Additionally, A13 treatment significantly reduced the mRNA levels of YAP-responsive genes *BIRC5* (Fig. 4C) and *ANKRD1* (Fig. 4D) in granulosa cells compared with those in untreated control. Yes-associated protein is a main transcriptional effector of Hippo signaling that binds TEAD in the nucleus to induce transcription of target genes. The results showed that A13 had no effect on the mRNA and protein levels of *YAP1* in granulosa cells compared with those in control (Fig. 4E to F). Lastly, the mRNA and

protein levels of *TEAD1* were tested. Surprisingly, at 10 uM, A13 increased the transcript levels of *TEAD1* in this cell type (Fig. 4G). The protein levels of TEAD1 were also increased after treatment with 10 μM of A13 (Fig. 4H) but reduced after treatment with 20 μM of A13 (Fig. 4I).

DISCUSSION

Primordial follicles in women remain dormant for several decades, and the mechanism of their activation is not completely understood. In vitro activation is an ongoing experimental technique used to assist patients with POI. Disruption of Hippo pathway signaling, which is important for organ size control and facilitates cell-cell contact growth and inhibition (32), has been shown to promote gonadotropin-independent follicle activation. Both biomechanical forces and biochemical alterations in the Hippo and PTEN/PI3K/Akt/FOXO3 pathways have been used to increase cellular growth factors in attempts to activate dormant primordial follicles. Prior studies of human ovarian tissue fragmentation alone, and combined with culture, have shown that Hippo pathway disruption induces the inhibitory pYAP to disappear in granulosa cells of primordial follicles, thus leading to an up-regulation of growth factors (9, 34, 39-42, 75).

The results of this study indicate that a COV434-TEAD luciferase reporter model may be useful to probe the early events of Hippo pathway signaling. Changes in cell density, matrix stiffness, and AKAP13 were able to alter RhoA, F-actin polymerization, Hippo pathway genes, YAP/TAZ DNA binding, and TEAD-luciferase reporter expression. The data show that TEAD-luc activity increased with decreased cell-cell contact, greater well stiffness (representing a surrogate of the ovarian tissue matrix), and treatment with AKAP13 activator (A02). TEAD-luciferase expression decreased with AKAP13 inhibitor (A13) treatment. No changes were found in TEAD-luc expression with AKAP13 overexpression; AKAP13 mutants GEF(-) and RII(-) of which both results may indicate that the endogenous AKAP13 levels are high in granulosa cells and compensate for the loss of function mutants; and FSH treatment. These results demonstrate that TEAD and the Hippo pathway are part of the gonadotropin-independent portion of folliculogenesis.

The mechanotransduction experiments were consistent with a study by De Roo et al. (75) who demonstrated that the Hippo pathway drove primordial follicle activation due to mechanical manipulation of human ovarian tissue that was cut into strips and cultured for 6 days. They noted a disappearance of pYAP in granulosa cells and an increase in nuclear YAP over increasing culture days and an up-regulation of *CTGF* expression. Additionally, higher TEAD-luc expression in stiffer substrate wells was consistent with previous data that showed that increasing collagen matrix stiffness can drive the nuclear accumulation of YAP and promote the activity of the YAP and TAZ transcriptional regulators in cancer-associated fibroblasts (76). These data may elucidate steps in the mechanism of mechanotransduction with ovarian tissue fragmentation and mechanical stress signaling.

The data indicate that A13 can consistently down-regulate YAP-responsive gene expression in granulosa cells by inhibiting AKAP13. By blocking the Rho-GEF activity of AKAP13 with A13, TEAD-luc activity was reduced in COV434 cells, consistent with inhibition of

YAP/TAZ activity. In the qPCR experiments, A13 treatment resulted in decreased mRNA levels of YAP-responsive genes *BIRC5* and *ANKRD1*. Although the results of *YAP1* and *TEAD1* in qPCR and Western blot were inconsistent, the overall data suggest a reduction in YAP-responsive gene expression by A13, suggesting a role of AKAP13-RhoA in Hippo signaling in granulosa cells. We extend the findings of Ohgushi et al. (51) and Diviani et al. (52) to granulosa cells and suggest that the mechanism of action of the inhibitory effect of A13 is via inhibiting the GEF region of AKAP13, which decreases RhoA-GTP and F-actin and turns on Hippo pathway genes, thus converting YAP to pYAP and ultimately leading to degradation. The decrease in cytoplasmic YAP then decreases nuclear YAP, which leads to decreased expression of CTGF/CCN2 and BIRC growth factors and inhibition of follicular growth.

In contrast to A13, A02 is thought to enhance the GEF activity of AKAP13, which increases RhoA-GTP and F-actin and turns off Hippo genes, thus converting fewer YAP to pYAP. This increase in stimulatory cytoplasmic YAP then crosses the nuclear membrane to increase nuclear YAP. The binding of YAP/TAZ to TEAD then leads to increased expression of CTGF/CCN2 and BIRC growth factors and possible increased follicular growth. Because no changes were detected upon transfection of the 2 AKAP13 mutants, GEF(-) and RII(-), additional studies with AKAP13 knockdown before transfecting the AKAP13 mutants may further elucidate and confirm whether the GEF region of AKAP13 is predominantly responsible for the changes in RhoA, YAP/TAZ, and TEAD expression.

Related to POI is fertility preservation, specifically ovarian tissue cryopreservation (OTC), which has emerged in both pediatric and adult populations with cancer or other diseases to mitigate the gonadotoxic effects of chemotherapy and radiation. The goal is to freeze and store oocytes within the tissue for transplantation in the future. This technique has been performed for over 25 years, and as of December 2019, the American Society for Reproductive Medicine announced that OTC is no longer considered experimental for patients receiving gonadotoxic treatments (77). Ovarian tissue cryopreservation is the only current option for fertility preservation in prepubertal girls and is also indicated for post-pubertal patients who do not have time for controlled ovarian hyperstimulation for oocyte cryopreservation. In 2004, the first successful live birth after autologous orthotopic transplantation of cryopreserved/thawed human ovarian tissue was reported (78). Since that time, over 360 transplantations and 130 live births have been reported in a 2017 study, but these numbers have likely increased to over 200 births in 2020 (79-81). It has been observed that it generally takes 60–240 days after autotransplantation for the ovarian tissue to regain its function (82-84), and it has the potential to last ≥7 years, depending on the following: age of the patient at the time of cryopreservation; diagnosis; baseline ovarian reserve; history of gonadotoxic treatment; freezing and thawing techniques; and cohort of primordial follicles transplanted (84-87). There are significant gaps in knowledge on how to increase the longevity of the tissue by either inhibition of primordial follicle activation before cryopreservation or methods of improving tissue perfusion and follicle activation after warming and reimplantation.

A significant number of follicles are lost during cryopreservation of ovarian tissue. Recent research has identified techniques for follicle protection/inhibition using a mTOR1/2

inhibitor, rapamycin, which is part of the PTEN/PI3K/Akt/FOXO3 signaling pathway (26-28). It is possible that patients who have diagnoses that put them at risk for POI due to gonadotoxic agents may benefit from primordial follicle inhibition before OTC to allow for fewer follicles to be lost, which is essential in populations who harbor a decreased number of follicles. Hence, potential uses of A13 or other small molecules that inhibit AKAP13 include culturing ovarian tissue immediately before cryopreservation for fertility preservation to counteract the activation by mechanotransduction that occurs during cutting of tissue into strips in preparation for freezing. This may minimize follicle loss due to fragmentation because a limitation of ovarian tissue transplantation after OTC requires revascularization of microvessels in the new tissue that can take up to 10 days after transplantation and results in a loss of two thirds of primordial follicles (88-90). The use of AKAP13 inhibitors may rescue follicles that would otherwise be lost. Such techniques may allow for future development of novel treatments to prevent accelerated follicle loss and may improve longevity of the ovarian tissue after transplant and increase the possibility of achieving pregnancy and live births. Further research is needed to better understand the changes these agents have on ovarian tissue and isolated ovarian follicles.

On the other hand, by promoting F-actin polymerization, A02 may act similarly to other primordial follicle activators that have been studied, including Jasplakinolide and sphingosine-1-phosphate, both of which promote actin polymerization in the ovary, leading to Hippo signaling disruption, nuclear localization of YAP, CTGF/CCN2 expression, and follicle growth (91). Potential uses for A02 or other small molecules that activate AKAP13 may include novel treatments for patients with POI after receiving gonadotoxic agents for cancer or bone marrow transplant for sickle cell disease; POI due to genetic causes, such as Turner syndrome, galactosemia, or fragile X premutation; idiopathic POI; and infertility due to diminished ovarian reserve or poor ovarian response to in vitro fertilization medications. Because POI is an issue of oocyte depletion or dysfunction (2), the use of AKAP13 activators could potentially activate the few remaining oocytes that patients with POI have to develop a mature oocyte for fertilization.

The limitations of these experiments include that they were performed on granulosa cells alone, whereas the ovary has multiple cell types, including the oocytes, theca cells, stromal cells, blood vessels, neurons, connective tissue, and ECM. The molecules and paracrine communication between all different cell types are important for function. Additionally, a granulosa tumor cell line may have inherent cellular proliferation properties that are different from normal follicular primordial granulosa cells. It is unknown whether similar effects would be seen on ovarian tissue cortex strips prepared for OTC or after thawing.

Thus, to confirm these results, future investigations should include testing primary granulosa cells from humans as well as culturing murine or human ovarian tissue in A13 and A02 to assess the mRNA and protein expression changes in whole tissue. Culturing ovarian tissue in A13 before cryopreservation could potentially counteract follicle activation and follicle loss that occurs during tissue processing by fragmentation before freezing or after transplantation. Additionally, for patients with POI, culturing ovarian tissue with A02 may be useful to activate follicles in vitro, may help mature an oocyte from a primordial

follicle through folliculogenesis to the metaphase II state, or promote follicle growth after transplantation.

In conclusion, these findings suggest that cell density and matrix stiffness play an important role in granulosa cell growth by mechanotransduction, which is in part mediated by the functions of AKAP13 and F-actin polymerization. The COV434-TEAD luciferase reporter model may be useful to probe the early events of Hippo pathway signaling, which promote primordial follicle inhibition/activation. Altering the Rho-GEF activity of AKAP13 with A13 and A02 led to the reduction and increase in TEAD-luc expression, respectively, which is upstream to the follicular growth factors. Together, these results support the hypothesis that the mechanotransduction and pharmacomanipulation of AKAP13 have a role in the Hippo pathway regulation of human granulosa cell growth and follicle activation. Novel treatments with AKAP13 activators and inhibitors may lead to the improved success of OTC and transplantation as well as potential treatments for POI.

Supplementary Material

Refer to Web version on PubMed Central for supplementary material.

Acknowledgments:

The authors thank Veronica Gomez-Lobo, M.D.; Anna Sokalska, M.D., Ph.D.; Mary B. Zelinski, Ph.D.; Sarina N. Hanfling, B.S.; Alexandra Chunovic, B.A.; and Kamaria Cayton Vaught, M.D.

Supported by a grant (ZIA #HD008985) from the National Institutes of Health, Bethesda, Maryland.

Supported by the Howard and Georgeanna Jones Endowment and grant (Z01-HD-008737-11) from the National Institute of Child Health and Human Development, National Institutes of Health, Bethesda, Maryland (to J.S.) and the Edward E. Wallach Research Award (to J.Y.M.).

REFERENCES

1. te Velde ER, Scheffer GJ, Dorland M, Broekmans FJ, Fauser BC. Developmental and endocrine aspects of normal ovarian aging. Mol Cell Endocrinol 1998;145:67–73. [PubMed: 9922101]
2. Kawashima I, Kawamura K. Disorganization of the germ cell pool leads to primary ovarian insufficiency. Reproduction 2017;153:R205–13. [PubMed: 28289071]
3. Cordeiro CN, Christianson MS, Selter JH, Segars JH Jr. In vitro activation: a possible new frontier for treatment of primary ovarian insufficiency. Reprod Sci 2016;23:429–38. [PubMed: 26787101]
4. Nelson LM. Clinical practice. Primary ovarian insufficiency. N Engl J Med 2009;360:606–14. [PubMed: 19196677]
5. Eshre Guideline Group on POI, et al. ESHRE guideline: management of women with premature ovarian insufficiency. Hum Reprod 2016;31:926–37. [PubMed: 27008889]
6. Massin N, Meduri G, Bachelot A, Misrahi M, Kuttenn F, Touraine P. Evaluation of different markers of the ovarian reserve in patients presenting with premature ovarian failure. Mol Cell Endocrinol 2008;282:95–100. [PubMed: 18191888]
7. Ernst EH, Grøndahl ML, Grund S, Hardy K, Heuck A, Sunde L, et al. Dormancy and activation of human oocytes from primordial and primary follicles: molecular clues to oocyte regulation. Hum Reprod 2017;32:1684–700. [PubMed: 28854595]
8. Novella-Maestre E, Herraiz S, Rodriguez-Iglesias B, Diaz-Garcia C, Pellicer A. Short-term PTEN inhibition improves in vitro activation of primordial follicles, preserves follicular viability, and restores AMH levels in cryopreserved ovarian tissue from cancer patients. PLoS One 2015;10:e0127786. [PubMed: 26024525]

9. Kawamura K, Cheng Y, Suzuki N, Deguchi M, Sato Y, Takae S, et al. Hippo signaling disruption and Akt stimulation of ovarian follicles for infertility treatment. Proc Natl Acad Sci U S A 2013;110:17474–9. [PubMed: 24082083]
10. Li J, Kawamura K, Cheng Y, Liu S, Klein C, Liu S, et al. Activation of dormant ovarian follicles to generate mature eggs. Proc Natl Acad Sci U S A 2010;107:10280–4 [PubMed: 20479243]
11. Reddy P, Liu L, Adhikari D,Jagarlamudi K, Rajareddy S, Shen Y, et al. Oocyte-specific deletion of Pten causes premature activation of the primordial follicle pool. Science 2008;319:611–3. [PubMed: 18239123]
12. Jagarlamudi K, Liu L, Adhikari D, Reddy P, Idahl A, Ottander U, et al. Oocyte-specific deletion of Pten in mice reveals a stage-specific function of PTEN/PI3K signaling in oocytes in controlling follicular activation. PLoS One 2009;4:e6186. [PubMed: 19587782]
13. Ding X, Zhang X, Mu Y, Li Y, Hao J. Effects of BMP4/SMAD signaling pathway on mouse primordial follicle growth and survival via up-regulation of Sohlh2 and c-kit. Mol Reprod Dev 2013;80:70–8. [PubMed: 23212987]
14. Tanwar PS, O'Shea T, McFarlane JR. In vivo evidence of role of bone morphogenetic protein-4 in the mouse ovary. Anim Reprod Sci 2008;106:232–40. [PubMed: 17644284]
15. Lee WS, Otsuka F, Moore RK, Shimasaki S. Effect of bone morphogenetic protein-7 on folliculogenesis and ovulation in the rat. Biol Reprod 2001;65:994–9. [PubMed: 11566718]
16. Huang EJ, Manova K, Packer AI, Sanchez S, Bachvarova RF, Besmer P. The murine steel panda mutation affects kit ligand expression and growth of early ovarian follicles. Dev Biol 1993;157:100–9. [PubMed: 7683280]
17. Yoshida H, Takakura N, Kataoka H, Kunisada T, Okamura H, Nishikawa SI. Stepwise requirement of c-kit tyrosine kinase in mouse ovarian follicle development. Dev Biol 1997;184:122–37. [PubMed: 9142989]
18. Tang K, Yang WC, Li X, Wu CJ, Sang L, Yang LG. GDF-9 and bFGF enhance the effect of FSH on the survival, activation, and growth of cattle primordial follicles. Anim Reprod Sci 2012;131:129–34. [PubMed: 22516229]
19. Kedem A, Fisch B, Garor R, Ben-Zaken A, Gizunterman T, Felz C, et al. Growth differentiating factor 9 (GDF9) and bone morphogenetic protein 15 both activate development of human primordial follicles in vitro, with seemingly more beneficial effects of GDF9. J Clin Endocrinol Metab 2011;96:E1246–54. [PubMed: 21632818]
20. Zhang P, Chao H, Sun X, Li L, Shi Q, Shen W. Murine folliculogenesis in vitro is stage-specifically regulated by insulin via the Akt signaling pathway. Histochem Cell Biol 2010;134:75–82. [PubMed: 20495820]
21. Kezele PR, Nilsson EE, Skinner MK. Insulin but not insulin-like growth factor-1 promotes the primordial to primary follicle transition. Mol Cell Endocrinol 2002;192:37–43. [PubMed: 12088865]
22. Ikeda Y, Hasegawa A, Tsubamoto H, Wakimoto Y, Kumamoto K, Shibahara H. Effects of gremlin-2 on the transition of primordial follicles during early folliculogenesis in the human ovary. Eur J Obstet Gynecol Reprod Biol 2016;203:72–7. [PubMed: 27267869]
23. Nilsson EE, Larsen G, Skinner MK. Roles of Gremlin 1 and Gremlin 2 in regulating ovarian primordial to primary follicle transition. Reproduction 2014;147:865–74. [PubMed: 24614542]
24. Nilsson EE, Kezele P, Skinner MK. Leukemia inhibitory factor (LIF) promotes the primordial to primary follicle transition in rat ovaries. Mol Cell Endocrinol 2002;188:65–73. [PubMed: 11911947]
25. Pankhurst MW. A putative role for anti-Müllerian hormone (AMH) in optimising ovarian reserve expenditure. J Endocrinol 2017;233:R1–13. [PubMed: 28130407]
26. Liu W, Zhang J, Wang L, Liang S, Xu B, Ying X, et al. The protective effects of rapamycin pretreatment on ovarian damage during ovarian tissue cryopreservation and transplantation. Biochem Biophys Res Commun 2021;534:780–6. [PubMed: 33162031]
27. Goldman KN, Chenette D, Arju R, Duncan FE, Keefe DL, Grifo JA, et al. mTORC1/2 inhibition preserves ovarian function and fertility during genotoxic chemotherapy. Proc Natl Acad Sci U S A 2017;114:3186–91. [PubMed: 28270607]

28. Zhang JM, Lu XL, Wang HX. Inhibition of mTORC1 signaling pathway is a valid therapeutic strategy in transplantation of cryopreserved mouse ovarian tissue. Cryo Letters 2020;41:38–43. [PubMed: 33973983]
29. Castrillon DH, Miao L, Kollipara R, Horner JW, DePinho RA. Suppression of ovarian follicle activation in mice by the transcription factor Foxo3a. Science 2003;301:215–8. [PubMed: 12855809]
30. Lee HN, Chang EM. Primordial follicle activation as new treatment for primary ovarian insufficiency. Clin Exp Reprod Med 2019;46:43–9. [PubMed: 31181871]
31. Halder G, Dupont S, Piccolo S. Transduction of mechanical and cytoskeletal cues by YAP and TAZ. Nat Rev Mol Cell Biol 2012;13:591–600. [PubMed: 22895435]
32. Gumbiner BM, Kim NG. The Hippo-YAP signaling pathway and contact inhibition of growth. J Cell Sci 2014;127:709–17. [PubMed: 24532814]
33. Grosbois J, Demeestere I. Dynamics of PI3K and Hippo signaling pathways during in vitro human follicle activation. Hum Reprod 2018;33:1705–14. [PubMed: 30032281]
34. Hsueh AJ, Kawamura K, Cheng Y, Fauser BC. Intraovarian control of early folliculogenesis. Endocr Rev 2015;36:1–24. [PubMed: 25202833]
35. Jorge S, Chang S, Barzilai JJ, Leppert P, Segars JH. Mechanical signaling in reproductive tissues: mechanisms and importance. Reprod Sci 2014;21:1093–107. [PubMed: 25001021]
36. Hornick JE, Duncan FE, Shea LD, Woodruff TK. Isolated primate primordial follicles require a rigid physical environment to survive and grow in vitro. Hum Reprod 2012;27:1801–10. [PubMed: 22456922]
37. Dupont S, Morsut L, Aragona M, Enzo E, Giulitti S, Cordenonsi M, et al. Role of YAP/TAZ in mechanotransduction. Nature 2011;474:179–83. [PubMed: 21654799]
38. Shah JS, Sabouni R, Cayton Vaught KC, Owen CM, Albertini DF, Segars JH. Biomechanics and mechanical signaling in the ovary: a systematic review. J Assist Reprod Genet 2018;35:1135–48. [PubMed: 29691711]
39. Suzuki N, Yoshioka N, Takae S, Sugishita Y, Tamura M, Hashimoto S, et al. Successful fertility preservation following ovarian tissue vitrification in patients with primary ovarian insufficiency. Hum Reprod 2015;30:608–15. [PubMed: 25567618]
40. Zhai J, Yao G, Dong F, Bu Z, Cheng Y, Sato Y, et al. In vitro activation of follicles and fresh tissue auto-transplantation in primary ovarian insufficiency patients. J Clin Endocrinol Metab 2016;101:4405–12. [PubMed: 27571179]
41. Fabregues F, Ferreri J, Calafell JM, Moreno V, Borrás A, Manau D, et al. Pregnancy after drug-free in vitro activation of follicles and fresh tissue autotransplantation in primary ovarian insufficiency patient: a case report and literature review. J Ovarian Res 2018;11:76. [PubMed: 30170634]
42. Kawamura K, Ishizuka B, Hsueh AJW. Drug-free in-vitro activation of follicles for infertility treatment in poor ovarian response patients with decreased ovarian reserve. Reprod Biomed Online 2020;40:245–53. [PubMed: 31753712]
43. Miller BT, Rubino DM, Driggers PH, Haddad B, Cisar M, Gray K, et al. Expression of brx proto-oncogene in normal ovary and in epithelial ovarian neoplasms. Am J Obstet Gynecol 2000;182:286–95. [PubMed: 10694326]
44. Rubino D, Driggers P, Arbit D, Kemp L, Miller B, Coso O, et al. Characterization of Brx, a novel Dbl family member that modulates estrogen receptor action. Oncogene 1998;16:2513–26. [PubMed: 9627117]
45. Welch EJ, Jones BW, Scott JD. Networking with AKAPs: context-dependent regulation of anchored enzymes. Mol Interv 2010;10:86–97. [PubMed: 20368369]
46. Zheng Y, Bender A, Cerione RA. Interactions among proteins involved in bud-site selection and bud-site assembly in Saccharomyces cerevisiae. J Biol Chem 1995;270:626–30. [PubMed: 7822288]
47. Diviani D, Soderling J, Scott JD. AKAP-Lbc anchors protein kinase A and nucleates Galpha 12-selective Rho-mediated stress fiber formation. J Biol Chem 2001;276:44247–57. [PubMed: 11546812]
48. Hall A. Rho GTPases and the actin cytoskeleton. Science 1998;279:509–14. [PubMed: 9438836]

49. Wettschureck N, Offermanns S. Rho/Rho-kinase mediated signaling in physiology and pathophysiology. J Mol Med (Berl) 2002;80:629–38. [PubMed: 12395147]
50. Rogers R, Norian J, Malik M, Christman G, Abu-Asab M, Chen F, et al. Mechanical homeostasis is altered in uterine leiomyoma. Am J Obstet Gynecol 2008;198:474.e1–11.
51. Ohgushi M, Minaguchi M, Sasai Y. Rho-signaling-directed YAP/TAZ activity underlies the long-term survival and expansion of human embryonic stem cells. Cell stem cell 2015;17:448–61. [PubMed: 26321201]
52. Diviani D, Raimondi F, Del Vescovo CD, Dreyer E, Reggi E, Osman H, et al. Small-molecule protein-protein interaction inhibitor of oncogenic Rho signaling. Cell Chem Biol 2016;23:1135–46. [PubMed: 27593112]
53. van den Berg-Bakker CA, Hagemeijer A, Franken-Postma EM, Smit VT, Kuppen PJ, van Ravenswaay Claasen HH, et al. Establishment and characterization of 7 ovarian carcinoma cell lines and one granulosa tumor cell line: growth features and cytogenetics. Int J Cancer 1993;53:613–20. [PubMed: 8436435]
54. Irving-Rodgers HF, Rodgers RJ. Extracellular matrix of the developing ovarian follicle. Semin Reprod Med 2006;24:195–203. [PubMed: 16944417]
55. Berkholtz CB, Lai BE, Woodruff TK, Shea LD. Distribution of extracellular matrix proteins type I collagen, type IV collagen, fibronectin, and laminin in mouse folliculogenesis. Histochem Cell Biol 2006;126:583–92. [PubMed: 16758163]
56. Zhao Y, Luck MR. Gene expression and protein distribution of collagen, fibronectin and laminin in bovine follicles and corpora lutea. J Reprod Fertil 1995;104:115–23. [PubMed: 7636792]
57. Sutovský P, Fléchon JE, Pavlok A. F-actin is involved in control of bovine cumulus expansion. Mol Reprod Dev 1995;41:521–9. [PubMed: 7576620]
58. Alexopoulos E, Shahid J, Ongley HZ, Richardson MC. Luteinized human granulosa cells are associated with endogenous basement membrane-like components in culture. Mol Hum Reprod 2000;6:324–30. [PubMed: 10729314]
59. Rodgers RJ, Vella CA, Rodgers HF, Scott K, Lavranos TC. Production of extracellular matrix, fibronectin and steroidogenic enzymes, and growth of bovine granulosa cells in anchorage-independent culture. Reprod Fertil Dev 1996;8:249–57. [PubMed: 8726863]
60. Carnegie JA. Secretion of fibronectin by rat granulosa cells occurs primarily during early follicular development. J Reprod Fertil 1990;89:579–89. [PubMed: 2119431]
61. Cottom J, Salvador LM, Maizels ET, Reierstad S, Park Y, Carr DW, et al. Follicle-stimulating hormone activates extracellular signal-regulated kinase but not extracellular signal-regulated kinase kinase through a 100-kDa phosphotyrosine phosphatase. J Biol Chem 2003;278:7167–79. [PubMed: 12493768]
62. Driggers PH, Segars JH, Rubino DM. The proto-oncoprotein Brx activates estrogen receptor beta by a p38 mitogen-activated protein kinase pathway. J Biol Chem 2001;276:46792–7. [PubMed: 11579095]
63. Oyen O, Myklebust F, Scott JD, Cadd GG, McKnight GS, Hansson V, et al. Subunits of cyclic adenosine 3',5'-monophosphate-dependent protein kinase show differential and distinct expression patterns during germ cell differentiation: alternative polyadenylation in germ cells gives rise to unique smaller-sized mRNA species. Biol Reprod 1990;43:46–54. [PubMed: 2393692]
64. Richards JS, Haddox M, Tash JS, Walter U, Lohmann S. Adenosine 3',5'-monophosphate-dependent protein kinase and granulosa cell responsiveness to gonadotropins. Endocrinology 1984;114:2190–8. [PubMed: 6327238]
65. Ratoosh SL, Richards JS. Regulation of the content and phosphorylation of RII by adenosine 3',5'-monophosphate, follicle-stimulating hormone, and estradiol in cultured granulosa cells. Endocrinology 1985;117:917–27. [PubMed: 2990878]
66. Diviani D, Abuin L, Cotecchia S, Pansier L. Anchoring of both PKA and 14-3-3 inhibits the Rho-GEF activity of the AKAP-Lbc signaling complex. EMBO J 2004;23:2811–20. [PubMed: 15229649]
67. Kino T, Souvatzoglou E, Charmandari E, Ichijo T, Driggers P, Mayers C, et al. Rho family guanine nucleotide exchange factor Brx couples extracellular signals to the glucocorticoid signaling system. J Biol Chem 2006;281:9118–26. [PubMed: 16469733]

68. Dong J, Feldmann G, Huang J, Wu S, Zhang N, Comerford SA, et al. Elucidation of a universal size-control mechanism in Drosophila and mammals. Cell 2007;130:1120–33. [PubMed: 17889654]
69. Garg H, Suri P, Gupta JC, Talwar G, Dubey S. Survivin: a unique target for tumor therapy. Cancer Cell Int 2016;16:49. [PubMed: 27340370]
70. Stein C, Bardet AF, Roma G, Bergling S, Clay I, Ruchti A, et al. YAP1 exerts its transcriptional control via TEAD-mediated activation of enhancers. PLoS Genet 2015;11:e1005465. [PubMed: 26295846]
71. Takahashi A, Seike M, Chiba M, Takahashi S, Nakamichi S, Matsumoto M, et al. Ankyrin repeat domain 1 overexpression is associated with common resistance to afatinib and osimertinib in EGFR-mutant lung cancer. Sci Rep 2018;8:14896. [PubMed: 30291293]
72. Livak KJ, Schmittgen TD. Analysis of relative gene expression data using real-time quantitative PCR and the 2(-delta delta C(T)) method. Methods 2001;25:402–8. [PubMed: 11846609]
73. Mayers CM, Wadell J, McLean K, Venere M, Malik M, Shibata T, et al. The Rho guanine nucleotide exchange factor AKAP13 (BRX) is essential for cardiac development in mice. J Biol Chem 2010;285:12344–54. [PubMed: 20139090]
74. Lipson KE, Wong C, Teng Y, Spong S. CTGF is a central mediator of tissue remodeling and fibrosis and its inhibition can reverse the process of fibrosis. Fibrogenesis Tissue Repair 2012;5(Suppl 1):S24. [PubMed: 23259531]
75. De Roo C, Lierman S, Tilleman K, De Sutter P. In-vitro fragmentation of ovarian tissue activates primordial follicles through the Hippo pathway. Hum Reprod Open 2020;2020:hoaa048. [PubMed: 33225076]
76. Calvo F, Ege N, Grande-Garcia A, Hooper S, Jenkins RP, Chaudhry SI, et al. Mechanotransduction and YAP-dependent matrix remodelling is required for the generation and maintenance of cancer-associated fibroblasts. Nat Cell Biol 2013;15:637–46. [PubMed: 23708000]
77. Practice Committee of the American Society for Reproductive Medicine. Fertility preservation in patients undergoing gonadotoxic therapy or gonadectomy: a committee opinion. Fertil Steril 2019;112:1022–33. [PubMed: 31843073]
78. Donnez J, Dolmans MM, Demylle D, Jadoul P, Pirard C, Squifflet J, et al. Live-birth after orthotopic transplantation of cryopreserved ovarian tissue. Lancet 2004;364:1405–10. [PubMed: 15488215]
79. Donnez J, Dolmans MM. Fertility preservation in women. N Engl J Med 2017; 377:1657–65. [PubMed: 29069558]
80. Dolmans MM, Donnez J. Fertility preservation in women for medical and social reasons: oocytes vs ovarian tissue. Best Pract Res Clin Obstet Gynaecol 2021;70:63–80. [PubMed: 32800711]
81. Andersen ST, Pors SE, Poulsen LC, Colmorn LB, Macklon KT, Ernst E, et al. Ovarian stimulation and assisted reproductive technology outcomes in women transplanted with cryopreserved ovarian tissue: a systematic review. Fertil Steril 2019;112:908–21. [PubMed: 31594631]
82. Donnez J, Dolmans MM, Pellicer A, Diaz-Garcia C, Sanchez Serrano M, Schmidt KT, et al. Restoration of ovarian activity and pregnancy after transplantation of cryopreserved ovarian tissue: a review of 60 cases of reimplantation. Fertil Steril 2013;99:1503–13. [PubMed: 23635349]
83. Schmidt KL,Andersen CY,Loft A,Byskov AG,Ernst E,Andersen AN. Follow-up of ovarian function post-chemotherapy following ovarian cryopreservation and transplantation. Hum Reprod 2005;20:3539–46. [PubMed: 16113042]
84. Kim SS. Assessment of long term endocrine function after transplantation of frozen-thawed human ovarian tissue to the heterotopic site: 10 year longitudinal follow-up study. J Assist Reprod Genet 2012;29:489–93. [PubMed: 22492223]
85. Gamzatova Z, Komlichenko E, Kostareva A, Galagudza M, Ulrikh E, Zubareva T, et al. Autotransplantation of cryopreserved ovarian tissue—effective method of fertility preservation in cancer patients. Gynecol Endocrinol 2014;30(Suppl 1):43–7. [PubMed: 25200829]
86. Silber SJ. Ovary cryopreservation and transplantation for fertility preservation. Mol Hum Reprod 2012;18:59–67. [PubMed: 22205727]

87. Andersen CY, Silber SJ, Bergholdt SH, Jorgensen JS, Ernst E. Long-term duration of function of ovarian tissue transplants: case reports. Reprod Biomed Online 2012;25:128–32. [PubMed: 22687323]

88. Christianson MS, Oktay K. Advances in fertility-preservation surgery: navigating new frontiers. Fertil Steril 2019;112:438–45. [PubMed: 31446903]

89. Oktay K, Bedoschi G, Pacheco F, Turan V, Emirdar V. First pregnancies, live birth, and in vitro fertilization outcomes after transplantation of frozen-banked ovarian tissue with a human extracellular matrix scaffold using robot-assisted minimally invasive surgery. Am J Obstet Gynecol 2016;214:94.e1–9.

90. Oktay K, Oktem O. Ovarian cryopreservation and transplantation for fertility preservation for medical indications: report of an ongoing experience. Fertil Steril 2010;93:762–8. [PubMed: 19013568]

91. Cheng Y, Feng Y, Jansson L, Sato Y, Deguchi M, Kawamura K, et al. Actin polymerization-enhancing drugs promote ovarian follicle growth mediated by the Hippo signaling effector YAP. FASEB J 2015;29:2423–30. [PubMed: 25690654]

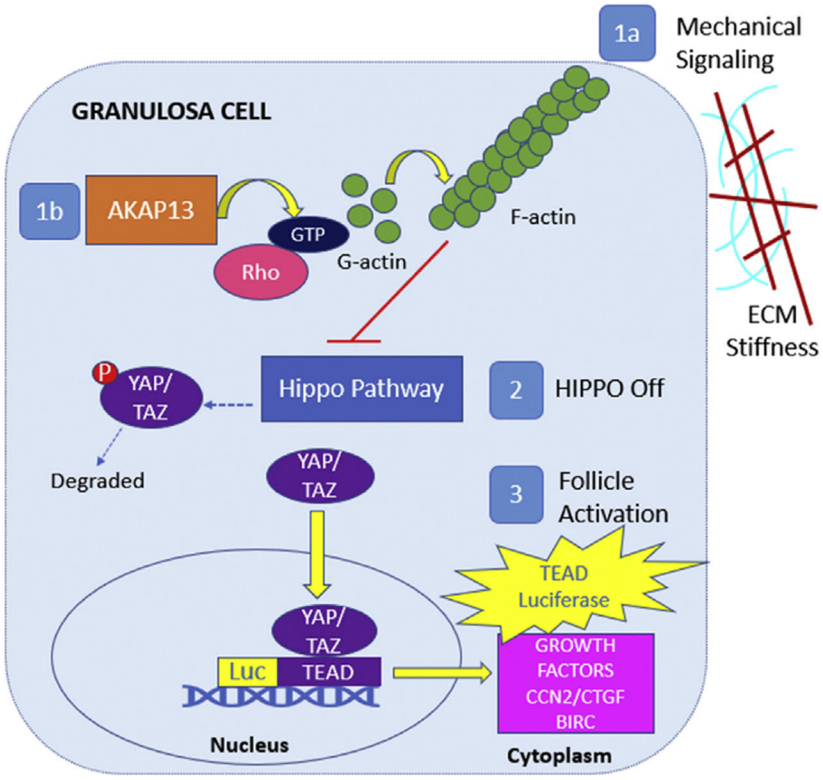

FIGURE 1.

Graphical abstract. In the granulosa cell, AKAP13 has a regulatory role in Rho activation and F-actin polymerization. (indicated as **1a**) Mechanical signaling, such as changes in cellular density and ECM stiffness, and (see **1b**) AKAP13 can promote F-actin polymerization, which turns off Hippo pathway genes (number 2) leading to YAP/TAZ migration into the nucleus to bind with TEAD (*red arrow*) and leads to an increase in cell growth factors (CCN2/ CTGF and BIRC, cellular proliferation, and follicle activation. To evaluate upstream changes of cell growth, transient transfection of a human granulosa tumor cell line with a TEAD-luc reporter was used to measure changes in nuclear YAP/TAZ deoxyribonucleic acid binding to TEAD and transcription of growth factors. AKAP13 = A-kinase anchoring protein 13; BIRC= baculoviral inhibitors of apoptosis repeat containing; CTGF= connective tissue growth factor; ECM = extracellular matrix; GTP = guanosine-5′-triphosphate; TAZ = transcriptional coactivator with PDZ-binding motif; TEAD = Tea domain family; TEAD-luc = TEAD luciferase; YAP = yes-associated protein.

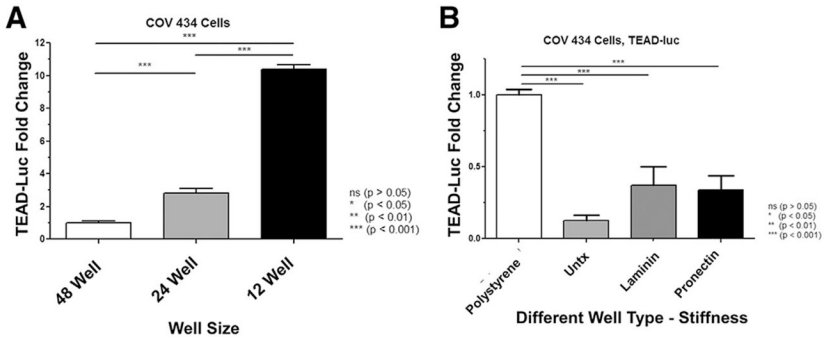

FIGURE 2.

Changes in mechanotransduction. (**A**) The well size increased Tea domain family (TEAD) activity. The same number of cells was placed into each well size, and additional medium was added in the 24-and 12-well plates to meet fluid volume requirements; thus, the lower the well plate number, the greater the well size, and the lower the cell density. The x-axis indicates increasing well size (48 wells, 200 μL/well; 24 wells, 500 μL/well; and 12 wells, 1,000 μL/well), and the y-axis shows TEAD-luciferase in RLU fold change. Increasing well size from 48-to 24-well plates, 24-to 12-well plates, and 48- to 12-well plates and decreased cell density resulted in an increase in normalized TEAD-luc activity. COV434 cells demonstrated a 2.8-fold (P<.001), 3.7-fold (P<.001), and 10.4-fold (P<.001) higher TEAD-luc activity, respectively. Samples were analyzed by n = 12 (48-well plate), 10 (24-well plate), and 9 (12-well plate) (2 biologic replicates). Error bars = standard error of the mean. Statistical analysis was performed using the Kruskal-Wallis test, followed by a post hoc Mann-Whitney U test. *P <.05, **P <.01, and ***P<.001. (**B**) Differences in TEAD-luc expression of granulosa cells when grown on plates with different stiffness and composition. To evaluate changes in mechanotransduction signaling, 4 different types of plates were compared. Polystyrene is the typical well type that is the stiffest with a rigidity of 2–4 GPa. Three types of Flexcell plates that were less stiff with a rigidity of 930 KPa with 3 different coatings were used: untreated, laminin, and ProNectin. The x-axis indicates different well types, and the y-axis shows TEAD-luciferase in RLU fold change. There was a significant decrease in TEAD-luc activity between the polystyrene plate and all 3 silicone Flexcell plates (P <.0001), meaning that there was greater reporter activity in cells plated on a stiffer matrix. There was no significant difference in TEAD-luc expression between untreated Flexcell plates and laminin- or ProNectin-coated plates (P =.24 and P =.13, respectively). Samples were analyzed with 2 biologic replicates and 3 technical replicates each. Error bars = standard error of the mean. Statistical analysis was performed using the Kruskal-Wallis test, followed by a post hoc Mann-Whitney U test. *P <.05, *P<.01, and ***P<.001. RLU = relative luciferase unit; TEAD = Tea domain family; TEAD-luc = TEAD luciferase.

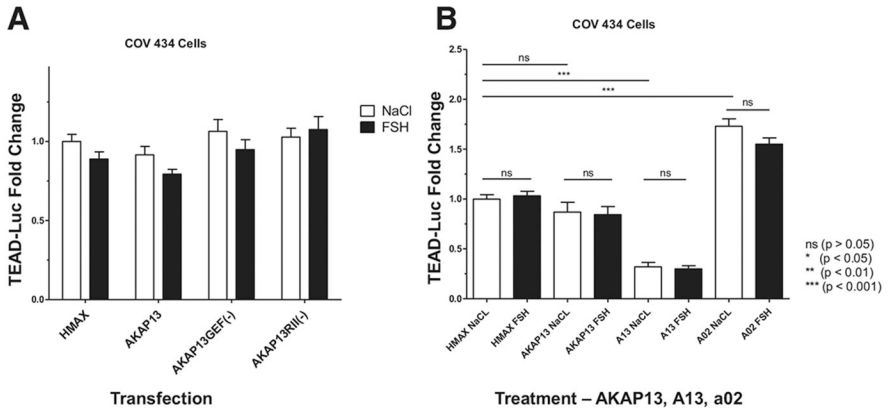

FIGURE 3.

A-kinase anchoring protein 13 manipulation. (**A**) No significant changes in TEAD-TEAD-luc expression with AKAP13 overexpression and AKAP13 mutants and with and without FSH treatment. The GEF-AKAP13 mutant, GEF(-), has a single point mutation: tyrosine to phenylalanine at position 2153 (Y2153F), which eliminates the GEF activity of AKAP13 and downstream Rho activity. The protein kinase A regulatory subunit II (RII)-AKAP13 mutant, RII(-), has 2 point mutations: alanine to proline at position 1251 and isoleucine to proline at position 1260 (A1251P/I1260P). This mutant disrupts binding of the RII regulatory subunit to AKAP13, thus interfering with activation of protein kinase A by AKAP13. The x-axis indicates the various vectors transfected into the COV434 cells, and the y-axis shows TEAD-luc in RLU fold change. White bars are cells treated with 0.9% NaCl, and black bars are cells treated with 1 IU of FSH (GONAL-f; Merck Serono, Darmstadt, Germany). No significant differences were found for the overall 2-way ANOVA or for each of the paired transfection comparisons between NaCl and FSH treatment. The results showing that there was no effect after treating with FSH support the idea that TEAD in the Hippo pathway is part of the gonadotropin-independent portion of folliculogenesis. There were also no differences between empty vector HMax-AKAP13 (HMax), AKAP13 overexpression, and GEF(-) or RII(-) mutant transfected cells treated with NaCl, which may indicate that the endogenous AKAP13 is already at its maximum use. Samples were analyzed with 3 biologic replicates and 3 technical replicates each. Error bars = standard error of the mean. Statistical analysis was performed using a permutation 2-way ANOVA followed by a post hoc quantile 1-way ANOVA to compare each pair of experimental groups. Data are presented with false discovery rate-adjusted *P* values. **P*<.05, ***P*<.01, and ****P*<.001. (**B**) The effect of A13 and A02 on TEAD-luc with AKAP13 overexpression plus either NaCl or FSH treatment. The x-axis indicates the vector transfected (HMax or AKAP13 overexpression) or treatment with the AKAP13 inhibitor (A13) or AKAP13 activator (A02) in COV434 cells. The y-axis shows TEAD-luc in RLU fold change. White bars are cells treated with 0.9% NaCl, and black bars are cells treated with 1 IU of FSH (GONAL-f; Merck Serono). Addition of AKAP13 did not augment TEAD-luc reporter activity, possibly due to high levels of endogenous AKAP13 in COV434 cells. Treatment with A13 reduced TEAD-luc activity by 68% (*P* <.0001), and treatment with A02 increased TEAD-luc activity by 73% (*P* <.0001). Samples were analyzed with 3 biologic replicates and 3 technical replicates each. Error bars = standard error of the

mean. Statistical analysis was performed using a permutation 2-way ANOVA followed by a post hoc quantile 1-way ANOVA to compare each pair of experimental groups where the permutation 2-way ANOVA results were statistically significant. Data are presented with false discovery rate-adjusted *P* values. **P*<.05, ***P*<.01, and ****P*<.001. . AKAP13 = A-kinase anchoring protein 13; ECM = extracellular matrix; FSH = follicle-stimulating hormone; GEF = guanine nucleotide exchange factor; GTP = guanosine-5′-triphosphate; RLU = relative luciferase unit; TEAD = Tea domain family; TEAD-luc = TEAD luciferase.

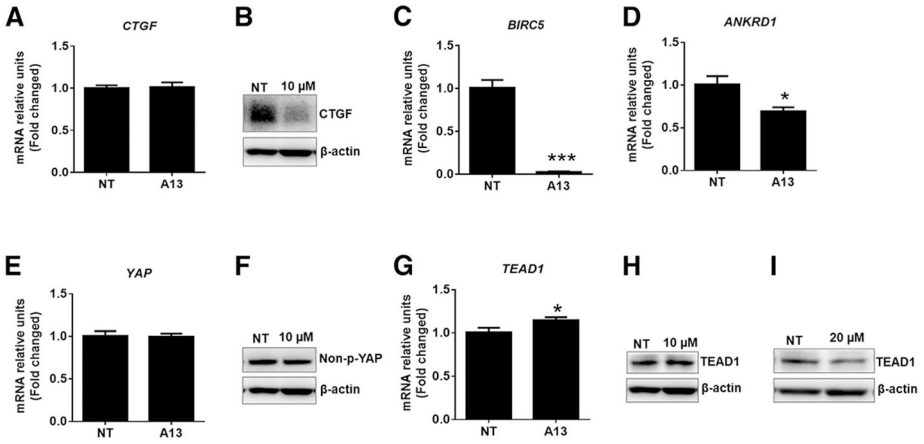

FIGURE 4.

Effect of A13 on Hippo signaling cascades in COV434 immortalized human granulosa cells. The x-axis is the cell condition of NT (control) or treated with the AKAP13 inhibitor (A13), and the y-axis is the mRNA relative unit fold change. Cells were treated with A13 at 10 or 20 μM for 24 hours. The mRNA and protein levels of several molecules of Hippo signaling by quantitative real-time polymerase chain reaction and Western blot were analyzed. (**A**) While the mRNA levels of *CTGF* YAP-responsive gene were unchanged, (**B**) CTGF protein levels were greatly reduced by A13 treatment. (**C** and **D**) *BIRC5* and *ANKRD1* are YAP-responsive genes that were also reduced by A13 treatment. The levels of (**E**) *YAP1* (a transcriptional effector of Hippo signaling) mRNA and (**F**) protein were unchanged after A13 treatment at 10 μM compared with untreated control. The (**G**) mRNA and (**H**) protein levels of *TEAD1* (a binding partner of YAP) were increased after A13 treatment at 10 μM, but (**I**) the protein levels of TEAD1 appear to be decreased by A13 at 20 μM. The mRNA and protein samples of *CTGF*, *YAP1*, and *TEAD1* were analyzed with 2 biologic replicates and 3 technical replicates each; those of *BIRC5* and *ANKRD1* were analyzed with 1 biologic replicate and 3 technical replicates. Error bars = standard error of the mean. For quantitative real-time polymerase chain reaction, a 1-way quantile ANOVA was used for analyses. $*P<.05$, $**P<.01$, and $***P<.001$. AKAP13 = A-kinase anchoring protein 13; ANKRD1 = ankyrin repeat domain 1;BIRC= baculoviral inhibitors of apoptosis repeat containing; CTGF= connective tissue growth factor; ECM = extracellular matrix; mRNA = messenger ribonucleic acid; NT= not treated; TEAD = Tea domain family; TEAD-luc = TEAD luciferase; YAP = yes-associated protein.